

4/1/86

OG 756

Subm. 12th International Conference on Neutrino
Physics and Astrophysics, Sendai, Japan, June 3-8, 1986

CONF-8606201-3
BNL 38469

Subm. XXIII International Conf. on High Energy Physics
16-23 July, 1986, Berkeley, CA

CONF-860701-13

MASTER

LIMITS ON NEUTRINO OSCILLATIONS IN THE

BNL--38469

FERMILAB NARROW BAND BEAM

DE86 015148

E.B. Brucker^{a)}, P.F. Jacques, M. Kalelkar, E.L. Koller^{a)},
R.J. Plano, and P.E. Stamer^{b)}

Rutgers University, New Brunswick, New Jersey 08903

N.J. Baker^{c)}, P.L. Connolly^{d)}, S.A. Kahn, M.J. Murtagh, and M. Tanaka

Brookhaven National Laboratory, Upton, New York 11973

C. Baltay, M. Bregman^{e)}, D. Caroumbalis^{f)}, L.D. Chen^{g)},
M. Hibbs^{e)}, P. Igo-Kemenes^{h)}, J.T. Liuⁱ⁾, J. Okamitsu^{j)},
G. Ormazabal^{k)}, A.C. Schaffer^{l)}, K. Shastri^{k)} and J. Spitzer^{h)}

Columbia University, New York 10027

- a) Permanent address: Stevens Institute of Technology, Hoboken, NJ.
- b) Permanent address: Seton Hall University, South Orange, NJ.
- c) Present address: Bear Stearns & Co., New York, NY.
- d) Deceased.
- e) Present address: IBM Thomas J. Watson Research Center, Yorktown Heights, NY.
- f) Present address: Lawrence Berkeley Laboratory, Berkeley, CA.
- g) Present address: AT&T Bell Laboratory, Allentown, PA.
- h) Present address: Heidelberg University, Heidelberg, W. Germany.
- i) Present address: Applied Physics Dept., Columbia University, NY, NY.
- j) Present address: Princeton University, Princeton, NJ.
- k) Present address: Bell Communication Research Inc., Red Bank, NJ.
- l) Present address: CERN, Geneva, Switzerland.

Abstract

A search for neutrino oscillations was made using the Fermilab narrow-band neutrino beam and the 15 ft. bubble chamber. No positive signal for neutrino oscillations was observed. Limits were obtained for mixing angles and neutrino mass differences for $\nu_{\mu} \rightarrow \nu_e$, $\nu_{\mu} \rightarrow \nu_{\tau}$, $\nu_e \rightarrow \nu_e$.

DISCLAIMER

This report was prepared as an account of work sponsored by an agency of the United States Government. Neither the United States Government nor any agency thereof, nor any of their employees, makes any warranty, express or implied, or assumes any legal liability or responsibility for the accuracy, completeness, or usefulness of any information, apparatus, product, or process disclosed, or represents that its use would not infringe privately owned rights. Reference herein to any specific commercial product, process, or service by trade name, trademark, manufacturer, or otherwise does not necessarily constitute or imply its endorsement, recommendation, or favoring by the United States Government or any agency thereof. The views and opinions of authors expressed herein do not necessarily state or reflect those of the United States Government or any agency thereof.

The existence of neutrino oscillations is an important question because it would imply a non-zero mass for at least one neutrino species and it would require that individual lepton numbers are not conserved. Many authors have reported on searches for neutrino oscillations in different energy regions.¹ This experiment relies on the ability of a heavy liquid bubble chamber to identify final state electrons and muons with good efficiency. The appearance of an excess number of events with electrons from a ν_μ beam could indicate neutrino oscillations. This collaboration, using a large statistics exposure of the Fermilab 15-foot bubble chamber to the wide band neutrino beam has published² upper limits for $\nu_\mu \rightarrow \nu_e$, $\nu_\mu \rightarrow \nu_\tau$ and $\nu_e \rightarrow \nu_e$ oscillations. These results relied on a subtraction of the ν_e flux from K_{e3} decays to obtain neutrino oscillation limits. The flux calculations depend on K/π production ratios, which are measured in other experiments. There are two advantages in performing this experiment with the narrow band neutrino beam. First, since interactions of neutrinos from $K_{\mu 2}$ decays can be separated from those from $\pi_{\mu 2}$ decay neutrinos, the expected ν_e flux determination depends only on the well known beam geometry and the well established $K_{e3}/K_{\mu 2}$ decay ratio. Secondly, the energy distribution of neutrino interactions from the 3-body K_{e3} decay neutrinos should look distinctly different from the spectrum of neutrino interactions from oscillations which will reflect the structure of the ν_μ spectrum from 2 body $\pi_{\mu 2}$ and $K_{\mu 2}$ decays.

To avoid the complexity of dealing with many parameters we consider oscillations between only two types of neutrinos at a time. In this case, the observed neutrino types, ν_α and ν_β , which are eigenstates of the weak current are quantum mechanical mixtures of the neutrino mass eigenstates ν_1 and ν_2 with masses m_1 and m_2 , respectively,

$$\nu_\alpha = \cos\theta \nu_1 + \sin\theta \nu_2$$

$$\nu_\beta = -\sin\theta \nu_1 + \cos\theta \nu_2$$

where θ is the single parameter describing the mixing between neutrino types. After traversing a distance l the probability of the appearance of ν_β from a beam that is initially pure ν_α is

$$P(\nu_\alpha \rightarrow \nu_\beta) = \sin^2(2\theta) \sin^2(1.27 \Delta m^2 l / E)$$

where $\Delta m^2 \equiv m_1^2 - m_2^2$ is in eV^2 , E is the neutrino energy in MeV and l is the distance from the source in meters. We observe experimentally the number of charge current interactions N_α of each species producing the corresponding charged lepton in the final state. To relate these N_α to the oscillation probability $P(\nu_\alpha \rightarrow \nu_\beta)$ we integrate over the decay space and the neutrino energy spectrum. The ratio is given by

$$R_{\alpha \rightarrow \beta} = \frac{N_\beta}{N_\alpha} = \frac{\iint P(\nu_\alpha \rightarrow \nu_\beta) \phi_\alpha \sigma_\beta dE dl}{\iint P(\nu_\alpha \rightarrow \nu_\alpha) \phi_\alpha \sigma_\alpha dE dl}$$

where $\phi_\alpha(E, l)$ is the initial ν_α flux and σ_α is the total charged current cross section for ν_α . For small oscillation probabilities $P(\nu_\alpha \rightarrow \nu_\alpha) \approx 1.0$ and this formula simplifies to

$$\Delta m^2 = \frac{(N_\beta/N_\alpha)^{1/2}}{\sin 2\theta (1.27 \langle \lambda/E \rangle)}$$

where $\langle \lambda/E \rangle^2 \equiv \iint (\lambda/E)^2 \phi_\alpha \sigma_\beta dE d\lambda / \iint \phi_\alpha \sigma_\alpha dE d\lambda$. For large Δm^2 many oscillation cycles occur within the detector and the $\sin^2 (1.27 \lambda/E \Delta m^2)$ term averages to 1/2 giving:

$$\sin^2(2\theta) = 2 \frac{N_\beta \iint \phi_\alpha \sigma_\alpha dE d\lambda}{N_\alpha \iint \phi_\alpha \sigma_\beta dE d\lambda}$$

If α and β represent μ and e the integrals cancel since the interaction cross sections σ_μ and σ_e are equal in the energy range of this experiment.

The data used in this experiment come from a 100000 picture exposure of the Fermilab 15 ft bubble chamber filled with a heavy Ne/H₂ mixture to the Fermilab narrow band beam with five momentum settings of the secondary meson beam: 120, 140, 165, 200, 250 GeV. The momentum bite for each setting is $\pm 10\%$. The momentum selected neutrinos are produced in a 400 meter decay region followed by a 1000 meter shield before the 15 ft bubble chamber. The beam is predominantly ν_μ from two body decays of K and π . In figure 1 the energy distribution for the charge current event sample is shown. The peak at 50 GeV is due to neutrino interactions from $\pi_{\mu 2}$ decays; a second peak at ≈ 130 GeV comes from neutrino interactions from $K_{\mu 2}$ decays. The principal background for neutrino oscillations is ν_e from $K_{e 3}$ decays, which are present at the level of 1% of the ν_μ events. Approximately 2.5% of the charged current events in the bubble chamber come from the wide band background component in the narrow band

beam.³ The expected ν_e contribution from the wideband background is negligible. The bubble chamber is approximately 4 meters in diameter and is contained within a 3 Tesla magnetic field. The liquid is an atomic mixture of 60% neon with 40% hydrogen. In this mixture the interaction length is ~ 125 cm and the radiation length is 40 cm. Hadrons will typically interact, muons will leave the chamber without interacting and electrons are reliably identified by their radiation. The identification of muons is aided by the two plane External Muon Identification System (EMI) behind the bubble chamber.

The pictures were scanned for events with an e^\pm in the final state. An electron was required to have at least two of the following signatures: (a) bremsstrahlung, (b) spiralization, (c) characteristic δ -ray, (d) tridents. The efficiency for detecting energetic electrons with $P_{e^-} > 2$ GeV/c was $(98 \pm 1)\%$. Each electron candidate was examined by a physicist. A restricted fiducial volume was imposed on the events to insure a high detection efficiency for the electron. The electron is required to have a momentum greater than 2 GeV/c to reduce the background from Compton scatters. A total of 7 events with $P_{e^-} > 2$ GeV/c and $E_\gamma > 10$ GeV were found in the fiducial volume. A single event with an electron and a muon verified by a two plane EMI signature was interpreted as a $\nu_\mu N \rightarrow \mu^- e^- X$ event and removed from this sample. The scanning efficiency for events with an electron was $(95 \pm 2)\%$.

In the same data sample 921 charged current events with $P_\mu > 2$ GeV/c and $E_\nu > 10$ GeV were found.⁴ Making an 11% correction⁴ for pion punchthrough from neutral current events we find 830 true charged current events. Because of the dichromatic property of the beam the muonic charged current events can be separated according to the parent pion or kaon decay. This is done using the quantity

$$S \equiv (E_m - E_\nu^\pi) / (E_\nu^K - E_\nu^\pi)$$

where E_m is the measured visible energy plus a correction for the missing neutral energy⁵; E_ν^π and E_ν^K are the theoretical energies obtained from the radial position in the chamber for neutrinos from $\pi_{\mu 2}$ and $K_{\mu 2}$ decays, respectively. Ideally one would expect $S = 0$. (1.) for $\pi(K)$ parents. The distribution is smeared by measurement errors in E_m , the decay position of the parent in the tunnel, and the momentum and angular dispersion of the parent beam. The S distribution of the muonic charged current sample is shown in figure 2. The separation into pion and kaon decay neutrinos is quite apparent. If we identify neutrino events from $\pi(K)$ decays as events with $S < 0.35$ (> 0.35), respectively, the misidentification of events is 2%. The ratio of events from $K_{\mu 2}$ to events from $\pi_{\mu 2}$ is 0.33 ± 0.03 .

The seven e^- events have the characteristics of ν_e charged currents. The $(y = (E_\nu - E_e)/E_\nu)$ distribution with the e^- interpreted as the outgoing lepton is consistent with being flat as it is expected to be for charged current neutrino interactions. In figure 3 the separation function S for the electron events is plotted. If the electron events were due to ν_e interactions where the ν_e arose from the oscillation of an original muon neutrino, then we would expect the distribution to be

similar to figure 2 with peaks at $S = 0, 1$ and a valley at $S = 0.3 - 0.5$. The dashed line in figure 3 indicates what S would look like for events from K_{e3} decays. The area under the curve is normalized to the expected K_{e3} background. This ν_{e3} background is calculated to be 6.0 ± 0.5 events from the observed number of $K_{\mu 2}$ events (210 ± 15), the $K_{e3}/K_{\mu 2}$ decay ratio ($7.6 \pm 0.1\%$) and the ratio of geometrical acceptance for the K_{e3} and $K_{\mu 2}$ decays which was determined using a Monte Carlo to be 40.2%. The events possessing an e^- are clearly consistent with coming from K_{e3} background. There is no evidence for neutrino oscillations and the data is used to set upper limits.

Correcting the observed events with an e^- for scanning and detection losses yields 7.35 events. The excess number of ν_e interactions that are not attributed to K_{e3} decays is therefore 1.35 ± 2.6 . Comparing this to the total number of ν_μ charge current interactions and assuming that the ν_e and ν_μ charge current cross sections are equal we have

$$R_{\mu \rightarrow e} < 5.6 \times 10^{-3} \text{ at } 90\% \text{ C.L.}$$

Using these same numbers, one can also set a limit on oscillations of the type $\nu_\mu \rightarrow \nu_\tau$. One looks for events of the type $\nu_\tau + Ne \rightarrow \tau^- + X$ where τ^- decays into $e^- \nu_\tau \bar{\nu}_e$. Using the measured branching ratio of 17% for this decay mode and the mean ratio of the cross sections, $\sigma_{\nu\tau}/\sigma_{\nu\mu}$, for narrow band neutrino energy distribution (0.77), we find

$$R_{\mu \rightarrow \tau} < 4.4 \times 10^{-2} \text{ at } 90\% \text{ C.L.}$$

Assuming that the K_{e3} decays provide a source of ν_e one can establish a limit on the disappearance of ν_e by comparing the observed number of ν_e events (7.3 ± 2.6) to the expected number (6.0 ± 0.5) events from the ν_e flux. The number of missing events is -1.3 ± 2.6 or less than

2.2 at 90% confidence level. This gives the limit on $P(\nu_e / \nu_e)$ to be less than $1.7/(1.7 + 6)$ or

$$R_e \rightarrow e < 0.27 \text{ at } 90\% \text{ C.L.}$$

The average $\langle \lambda/E \rangle = 0.023 \text{ m/MeV}$ (corresponding to $\langle 1/E^2 \rangle^{-1/2} = 50.7 \text{ GeV}$). Using $\langle \lambda/E \rangle$ the limits on oscillations at small Δm^2 are

$$\sin(2\theta) \Delta m^2 < 2.5 \text{ eV}^2 \text{ for } \nu_\mu \rightarrow \nu_e$$

$$\sin(2\theta) \Delta m^2 < 8.1 \text{ eV}^2 \text{ for } \nu_\mu \rightarrow \nu_\tau \text{ at } 90\% \text{ C.L.}$$

$$\sin(2\theta) \Delta m^2 < 18.8 \text{ eV}^2 \text{ for } \nu_e \rightarrow \nu_e$$

For the last number we used $\langle \lambda/E \rangle = 0.0197 \text{ m/MeV}$ corresponding to the higher E_ν spectrum from K_{e3} decays. For very large Δm^2 the ratio limits can be interpreted as limits on the oscillation angle:

$$\sin^2(2\theta) < 0.011 \text{ for } \nu_\mu \rightarrow \nu_e$$

$$\sin^2(2\theta) < 0.088 \text{ for } \nu_\mu \rightarrow \nu_\tau \text{ at } 90\% \text{ C.L.}$$

$$\sin^2(2\theta) < 0.54 \text{ for } \nu_e \rightarrow \nu_e$$

This experiment can be compared to a similar one with much higher statistics² performed by the same collaboration in the Fermilab wide band beam. The primary difference is that the systematic uncertainty in the flux calculation limits the accuracy of the wide band results whereas in this experiment the statistical errors dominate. Figure 4 compares the upper limits obtained for oscillations in the two experiments.

In the small Δm^2 region the limit is proportional to the reciprocal root mean square of the neutrino energy. Since the wide band beam is lower in average energy than the narrow band beam, the wide band limits are better at small Δm^2 . However the a priori sensitivity (independent of the actual fluctuations) of the two experiments are similar in the large Δm^2 region.

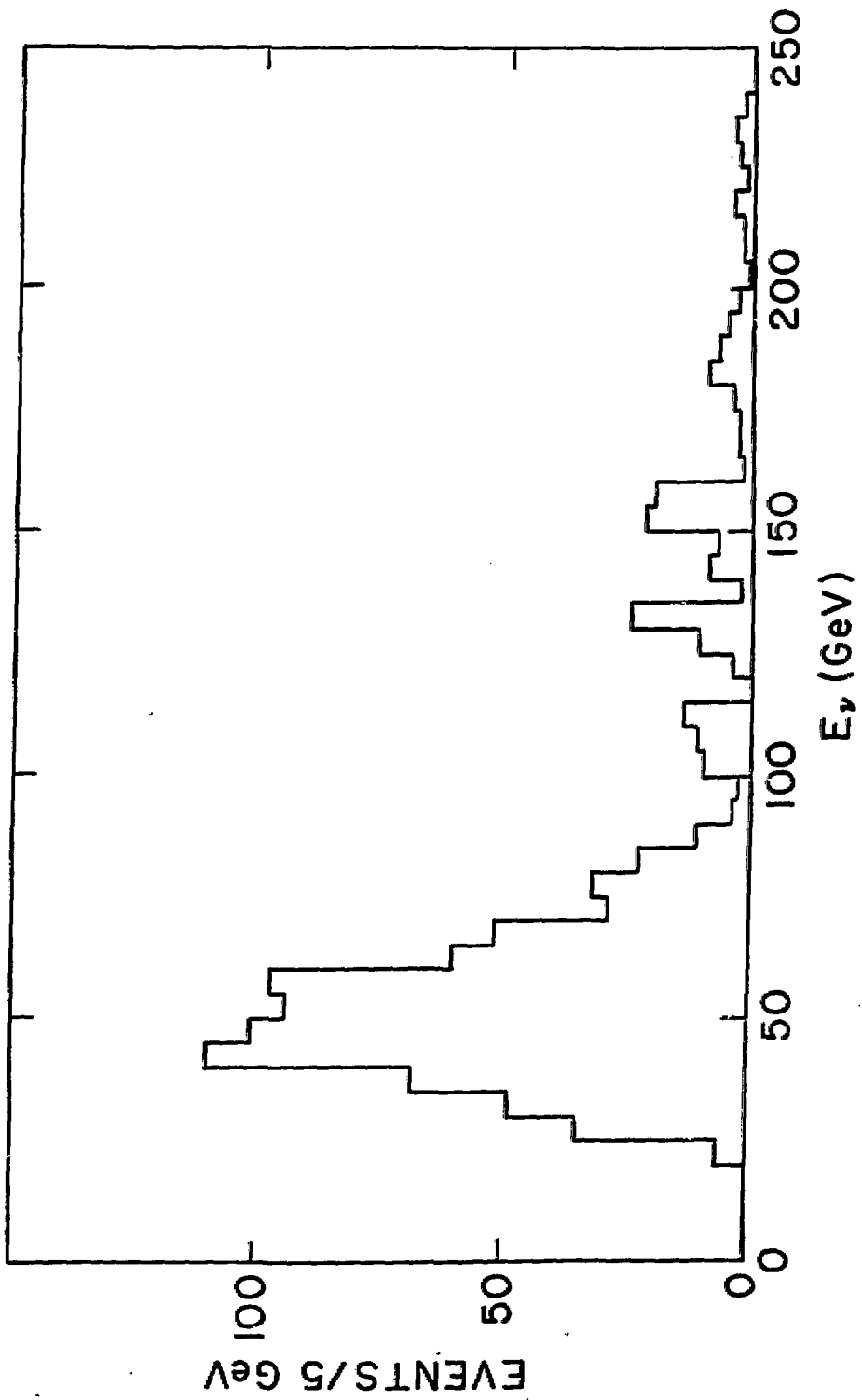
We would like to thank the people in the Neutrino Laboratory at Fermilab and the scanning and measuring staffs at Brookhaven National Laboratory, Columbia University, and Rutgers University, whose hard work has made this experiment possible. This research is supported by the U.S. Department of Energy (contract DE-AC02-76CH0016) and the National Science Foundation.

References

1. The current status was reviewed by C. Baltay at Neutrino '82 (Proc. NEUTRINO 82 - supplement, 14-19 June 1982, Balatonfüred, Hungary, p.9). This article provides a comprehensive list of references.
2. N.J. Baker et. al., Phys. Rev. Lett. 47 1576 (1981).
3. R. Blair et al., Nucl. Instr. & Meth. 226, 281 (1984).
4. N.J. Baker et. al., Phys. Rev. Lett. 51 735 (1983).
5. We correct for the missing neutral energy by increasing the visible hadronic energy by 13%, a correction factor determined by using transverse momentum balance on the ensemble of events.

Figures

1. Energy distribution of charge current events in the Narrow Band Experiment.
2. The separation function S for the muonic charge current data sample. Events from $\pi^+ \rightarrow \mu^+ \nu_\mu$ and $K^+ \rightarrow \mu^+ \nu_\mu$ are clustered at $S=0$ and 1, respectively. The dashed lines indicate fits to the $\pi_{\mu 2}$ and $K_{\mu 2}$ events in the ambiguous region. The solid curve is the fitted sum of $\pi_{\mu 2}$ and $K_{\mu 2}$ events.
3. Separation function S for events with an electron. The superimposed curve illustrates the theoretical distribution from K_{e3} decays.
4. $\sin^2 2\theta$ vs. Δm^2 for $\nu_\mu \rightarrow \nu_e$, $\nu_\mu \rightarrow \nu_\tau$ and $\nu_e \rightarrow \nu_e$. The wide band limits are shown as dashed lines for comparison.



NUMBER OF EVENTS

